Available online at www.sciencedirect.com
ScienceDirect
Bioorganic & Medicinal Chemistry Letters 17 (2007) 5989–5994
Bioorganic & Medicinal Chemistry Letters

Optimization of a pyrazoloquinolinone class of Chk1 kinase inhibitors

Edward J. Brnardic,[a,*] Robert M. Garbaccio,[a] Mark E. Fraley,[a] Edward S. Tasber,[a] Justin T. Steen,[a] Kenneth L. Arrington,[a] Vadim Y. Dudkin,[a] George D. Hartman,[a] Steven M. Stirdivant,[b] Bob A. Drakas,[b] Keith Rickert,[b] Eileen S. Walsh,[b] Kelly Hamilton,[b] Carolyn A. Buser,[b] James Hardwick,[b] Weikang Tao,[b] Stephen C. Beck,[b] Xianzhi Mao,[b] Robert B. Lobell,[b] Laura Sepp-Lorenzino,[b] Youwei Yan,[c] Mari Ikuta,[c] Sanjeev K. Munshi,[c] Lawrence C. Kuo[c] and Constantine Kreatsoulas[d]

[a]*Department of Medicinal Chemistry, Merck Research Laboratories, West Point, PA 19486, USA*
[b]*Department of Cancer Research, Merck Research Laboratories, West Point, PA 19486, USA*
[c]*Department of Structural Biology, Merck Research Laboratories, West Point, PA 19486, USA*
[d]*Department of Molecular Systems, Merck Research Laboratories, West Point, PA 19486, USA*

Received 17 April 2007; revised 3 July 2007; accepted 17 July 2007
Available online 19 August 2007

Abstract—The development of 2,5-dihydro-4H-pyrazolo[4,3-*c*]quinolin-4-ones as inhibitors of Chk1 kinase is described. Introduction of a fused ring at the C7/C8 positions of the pyrazoloquinolinone provided an increase in potency while guidance from overlapping inhibitor bound Chk1 X-ray crystal structures contributed to the discovery of a potent and solubilizing propyl amine moiety in compound **52** (Chk1 IC_{50} = 3.1 nM).

Although effective, DNA damaging agents used in chemotherapy are considered to be less than optimal in that they show little selectivity for killing tumor cells over normal proliferating cells. In response to DNA damage, a normal cell activates checkpoints that delay cell cycle transitions via the tumor suppressor protein p53 and the checkpoint kinase Chk1, respectively. This delay allows the cell to repair DNA before entering into mitosis.[1–4] Many tumor cells, however, lack G1- and S-phase checkpoints due to inactivation of the p53 tumor suppressor gene (estimated 50–70% of all cancers), and rely solely on Chk1 for arrest and repair. In these DNA damaged tumor cells, Chk1 inhibition results in abrogation of cell cycle arrest and allows premature mitotic entry ultimately leading to cell death through mitotic catastrophe and apoptotic pathways. Chk1 inhibitors should therefore sensitize tumor cells deficient in p53 to DNA damaging agents.[5,6] In this paper we report efforts to maximize the potency of lead **1** (Fig. 1).

Our lead optimization efforts were initially guided by the overlay of the X-ray crystal structures of Chk1 with bound inhibitors **1** and **2** (Figs. 1 and 2).[7] The X-ray crystal structures of **1** and **2** indicated that both leads

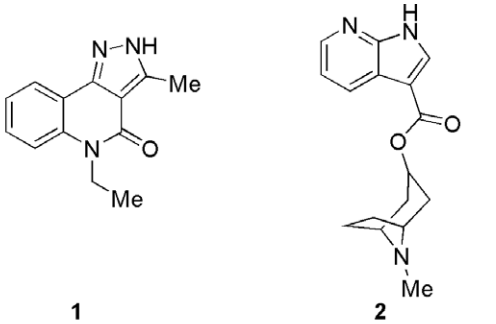

1
Chk1 IC_{50} = 980 nM

2
Chk1 IC_{50} = 660 nM

Figure 1. Leads **1** and **2**.

Keywords: Chk1 kinase; Pyrazoloquinolinone; Oncology; Checkpoint escape; DNA damage.
* Corresponding author. E-mail: edward_brnardic@merck.com

0960-894X/$ - see front matter © 2007 Elsevier Ltd. All rights reserved.
doi:10.1016/j.bmcl.2007.07.051

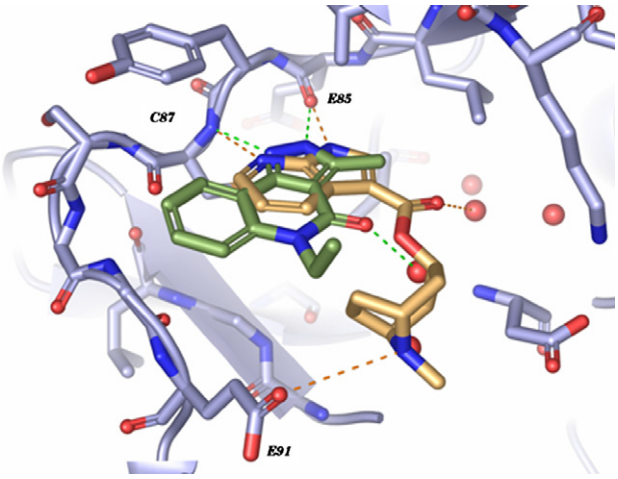

Figure 2. X-ray crystal structure with bound inhibitors **1** and **2**.

were anchored to the adenine region[8] of the Chk1 ATP binding site through hydrogen bonds to the peptide backbone at Glu85 and Cys87. Analysis and comparison of the bound structures for **1** and **2** indicated three strategies for rapid optimization of potency in **1**. The first strategy aimed to fill an evident hydrophobic pocket located between the aryl ring of **1** and the protein–solvent interface. The second strategy focused on the introduction of polar groups designed to drive potency enhancement by interaction with the solvent front and improve aqueous solubility. The final, and most provocative, strategy was suggested by the ionic interaction of the tropane amine **2** with Glu91, an interaction not utilized by **1**. It was surmised that substitution on the 4-, 5- or 6-positions of the pyrazoloquinolinone ring had the potential to reach this key residue (Glu91).

To explore our first strategy[9] we utilized anthranilic acids[10,11] to prepare our target molecules (Fig. 3). Substituted anthranilic acids **3** were cyclized with ethyl chloroacetate to provide benzoxazinones **4**. These electrophiles reacted with the sodium anion of ethyl acetoacetate to provide acrylates **5** which were cyclized and decarboxylated upon treatment with sodium methoxide to provide 4-hydroxyquinolinones **6**. Heating the 4-hydroxyquinolinones **6** with hydrazine afforded the pyrazoloquinolinones **7** in good overall yield.

The initial set of compounds (Table 1) established the optimal vector for filling this hydrophobic pocket. Substitution at the 9-position was not tolerated as both the 9-methyl (**14**) and 9-chloro (**15**) derivatives were inactive.[12,13] We rationalized that the substituent at the 9-position collides with the hinge region of the ATP pocket preventing the key hydrogen bonding interactions with the peptide main chain. We were also unable to improve activity with substitution at the 6- and 7-positions, as compounds **9** and **10** showed no

Table 1. Inhibitory activity of aryl modifications (**8**–**17**)

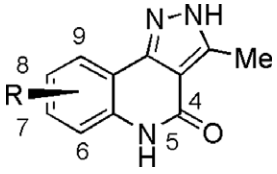

Cmpd	R	Chk1 IC_{50} (nM)	Cell EC_{50}(nM)
8	H	1370	
9	6-Me	1490	
10	7-CI	1980	
11	8-Me	230	
12	8-CI	40	2980
13	8-$NHCOCH_3$	7080	
14	9-Me	>100,000	
15	9-CI	28,860	
16	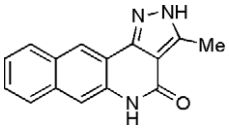	29	710
17	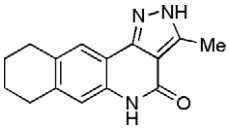	130	1210

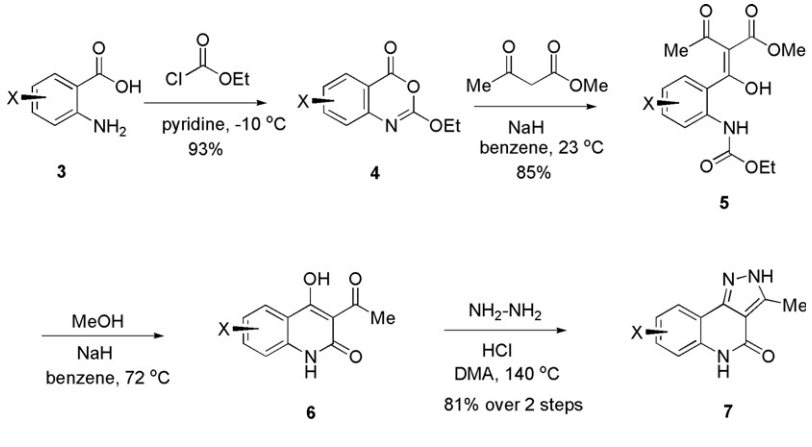

Figure 3. Synthesis of pyrazoloquinolinones from anthranilic acids.

significant change in potency. Substitution at the 8-position was identified as the key position for improving potency.[14] The methyl derivative **11** offered a 6-fold increase, while the chloro derivative **12** provided a greater than 30-fold increase in potency. As predicted, polar groups such as the 8-amide (**13**) were less tolerated in the hydrophobic pocket in that they displayed a significant loss of potency. We were, however, pleased to find that the 7,8-fused ring systems of **16** and **17** greatly enhanced enzyme potency (up to 50-fold) and showed modest levels of cell activity.[15]

With the identification of potent cores via these modifications we turned our attention to our second strategy. Molecular modeling suggested that substitution on the fused cyclohexyl ring could project into solvent and substituents might be used to modify properties such as solubility without detrimentally affecting enzyme affinity. We prepared analogs with polar groups at the solvent front utilizing the reaction scheme shown in Figure 4. The nitrobenzene derivative **18** was Cbz-protected to give **19** which was then reduced to aniline **20** with stannous (II) chloride. Aniline **20** was iodinated with NIS to provide a 1:2 mixture of iodo-isomers from which the minor, desired *ortho*-iodoaniline **21** was isolated by chromatography. Coupling reactions of iodoaniline **21** with protected pyrazole-4-carboxylic acids[16] **22** using PyClu[17] provided amide **23**, which was alkylated with ethyl bromide in the presence of cesium carbonate in good yield. The tertiary amide **24** underwent Heck cyclization[18] at 90 °C to provide protected pyrazoloquinolinones **25**. Removal of the Cbz-protecting group under hydrogenolysis conditions provided amine **26** which could be elaborated with an electrophile to provide **27**.

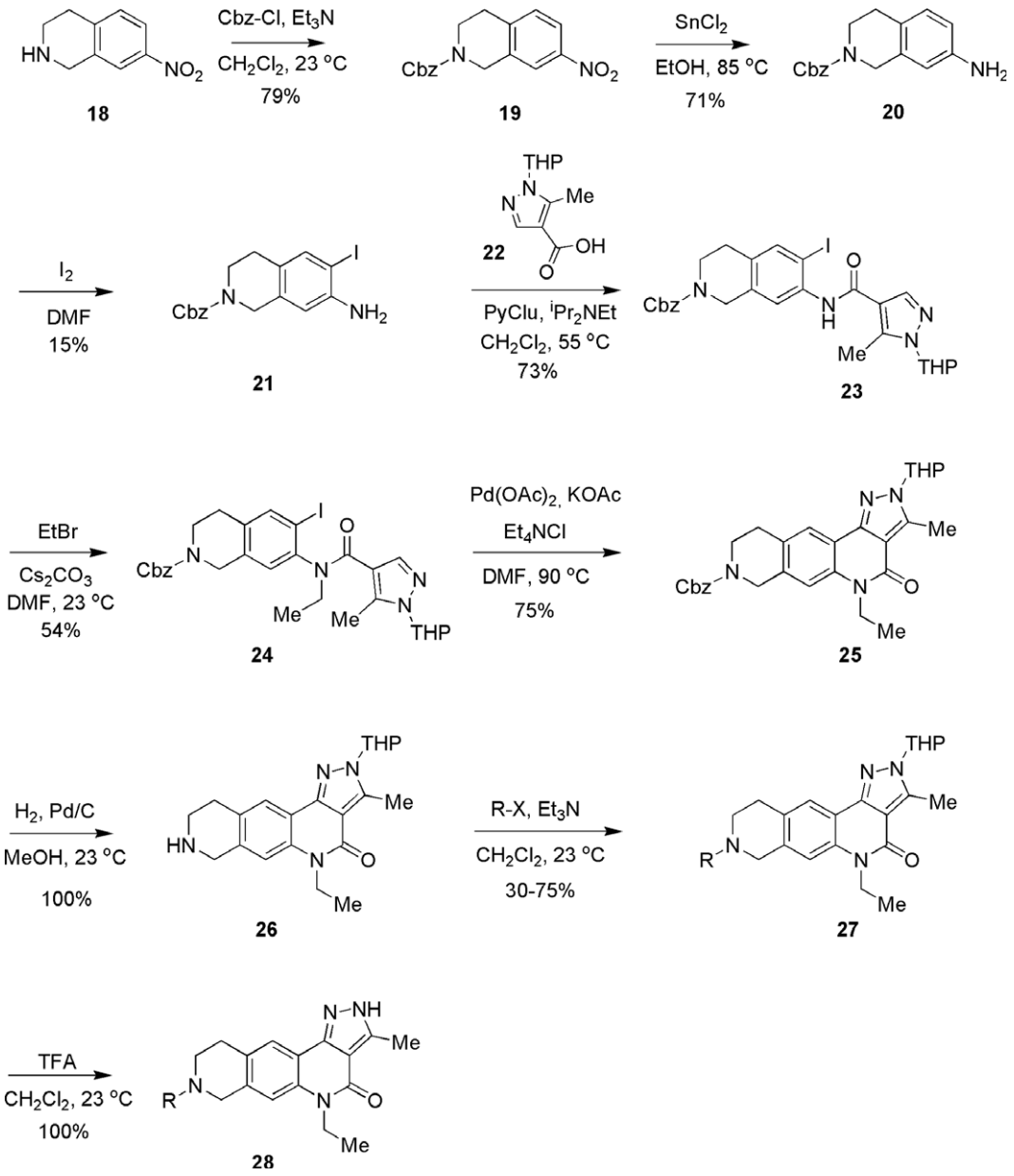

Figure 4. Synthesis of pyrazoloquinolinones from anilines.

Table 2. Inhibitory activity of compounds with polar groups at the solvent front (**29**–**31**)

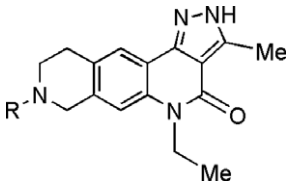

Cmpd	R	Chk1 IC_{50} (nM)	Cell EC_{50} (nM)	PSA(Å^2)
29	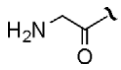	18	>10,000	103
30	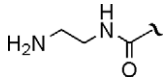	12	>10,000	115
31	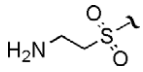	10	>10,000	123

The pyrazoloquinolinone was then deprotected using trifluoroacetic acid to provide **28**.

Our strategy to improve enzyme potency and aqueous solubility through the introduction of polar groups designed to reach the solvent front was successful. Compounds **29**–**31** displayed enhanced aqueous solubility and were found to be ~10-fold more potent than the comparison compound **17**.[19] However, these compounds (**29**–**31**) were found to be inactive in our cell-based assay, presumably due to poor cellular permeability[20] that may be a result of their high polarity (PSA > 100 Å^2)[21] (Table 2).

Our third strategy focused on an attempt to reach the key residue Glu91. Molecular modeling suggested the possible interaction of Glu91 with substitution from the 4-, 5-, or 6-positions. We explored this possibility using cores **12**, **16**, and **17**. The synthesis of our targets employed a variety of reaction sequences. The alkylation of pyrazoloquinolinones **32**[22] with alkylating agents and cesium carbonate (Fig. 5) yielded a 3:1 mixture of N-alkylated (**33**) versus O-alkylated (**34**) products which were separated by silica gel chromatography. In order to substitute the 4-position, the quinolinones were converted to chloroquinolinones[23] **35** by heating with $PhPOCl_2$. Chlorides **35** were then reacted with amines to afford aminoquinolinones **36**. Compounds **38** were derived from Suzuki coupling reactions with the tetrahydronaphthyl aryl bromide[24] **37** and the appropriate boronic acid (Fig. 6), followed by further derivitization as required.

Analysis of SAR (Table 3) indicated that substitution at the 4- and 6-positions (**39**–**44**) did not provide improvement in activity, indicating that the side chains were not able to make productive interactions within the ATP pocket. Gratifyingly, we found that substitution on the 5-position provided a significant increase in activity. A three-carbon amine chain was found to be optimal (**46**),[25] as neither the two-carbon (**45**) nor the four-carbon (**47**) chain lengths provided equivalent potency enhancement. Application of the propyl amine chain to cores **16** and **17** gave compounds **48** and **49** which showed excellent enzyme and cell-based potency.[26] Since **49** displayed superior solubility properties to analog **48**, we focused on derivatives employing the tetrahydronaphthyl core. While **49** showed excellent potency and

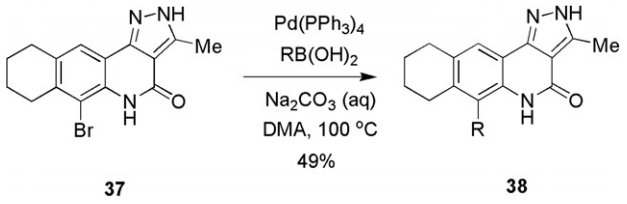

Figure 6. Synthesis of 6-substituted pyrazoloquinolinones.

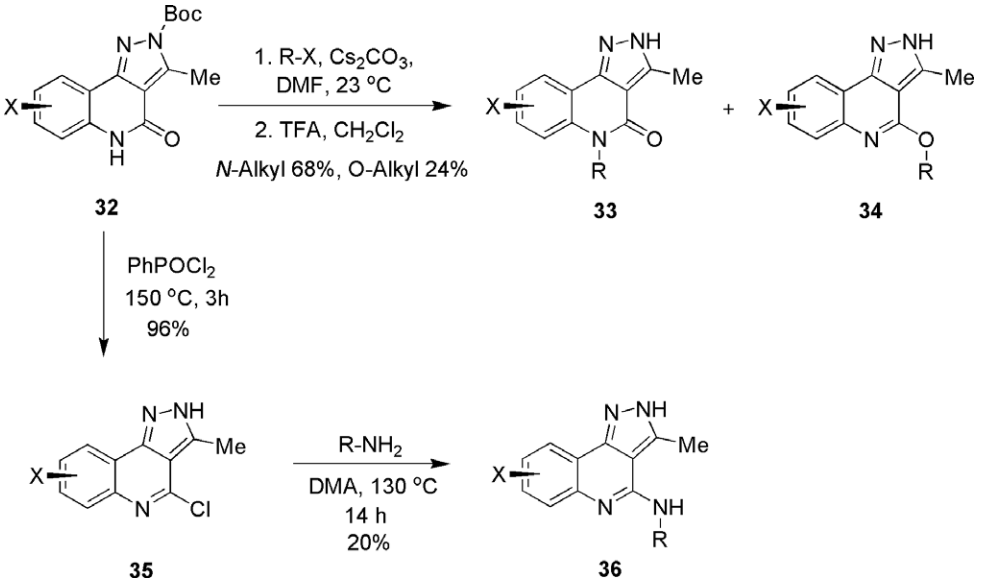

Figure 5. Synthesis of 4- and 5-substituted pyrazoloquinolinones.

Table 3. Inhibitory activity of compounds designed to access Glu91

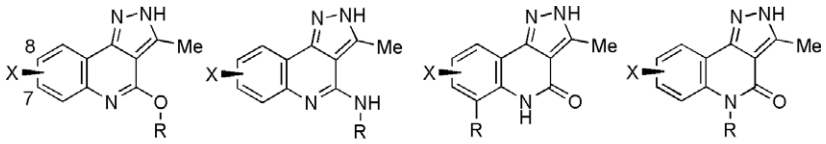

C D E F

Cmpd	X	Structure	R	Chk1 IC_{50} (nM)	Cell EC_{50} (nM)
39	8-CI	C	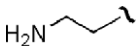	850	
40	8-CI	C	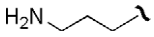	64	10,180
41	8-CI	D	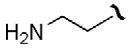	60	
42	8-CI	D	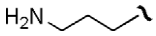	220	
43	7, 8-Cy	E	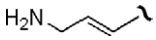	58	
44	7, 8-Cy	E	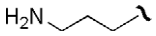	290	
45	8-CI	F	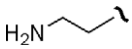	36	980
46	8-CI	F	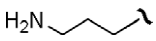	1.2	160
47	8-CI	F	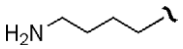	20	1010
48	7, 8-Cy	F	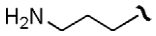	0.66	15
49	7, 8-Cy	F	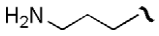	1.1	94
50	7, 8-Cy	F	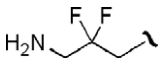	14	1290
51	7, 8-Cy	F	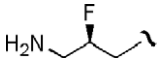	3.2	83
52	7, 8-Cy	F	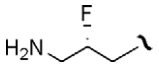	3.1	65

aqueous solubility, it demonstrated moderate binding to the I_{Kr} potassium channel hERG (human *Ether-a-go-go* Related Gene)[27] with an IC_{50} = 5300 nM.[28] We sought to decrease the hERG activity by reducing the basicity of the amine functionality[29] of **49** (pK_a = 10.2).[30] Specifically, we investigated modulating basicity through the introduction of fluorine in the propyl chain (**50**–**52**).[31] The difluoro derivative **50** (pK_a = 7.6) suffered a reduction in potency perhaps as a result of a diminished ionic interaction with Glu91. However, the mono fluoro derivative **52** (pK_a = 8.9) maintained good cell potency (EC_{50} = 65 nM) and showed a modest improvement in hERG off-target activity (IC_{50} = 13,200 nM).

In summary, we have described the use of X-ray crystallography to rapidly optimize Chk1 potency (>1000-fold improvement) from an HTS lead. Through the comparison of two X-ray structures of HTS leads **1** and **2**,

potential hydrophobic and ionic interactions were identified. This effort culminated in the fusion of a cyclohexyl ring and appendage of a propyl amine at N-5 to produce inhibitor **52** with excellent Chk1 potency and solubility properties.

Acknowledgment

We thank Carl Homnick for chiral separations of intermediates to give **51** and **52**.

References and notes

1. Bartek, J.; Lukas, J. *Cancer Cell* **2003**, *2*, 421.
2. Zhou, B. S.; Bartek, J. *Nat. Rev. Cancer* **2004**, *4*, 1.
3. Tao, Z.; Lin, N. *Anti-Cancer Agents Med. Chem.* **2006**, *6*, 377.
4. Hapke, G.; Yin, M. B.; Rustum, Y. M. *Cancer Metastasis Rev.* **2001**, *20*, 109.
5. Kawabe, T. *Mol. Cancer Ther.* **2004**, *3*, 513.
6. Prudhomme, M. *Recent Patents Anti-Cancer Drug Discov.* **2006**, *1*, 55.
7. PDB coordinates for **1**: 2QHN, **2**: 2QHM.
8. Traxler, P.; Furet, P. *Pharmacol. Ther.* **1999**, *82*, 195.
9. For full experimental detail on compounds described in this paper, see WO2006074281.
10. Mitsos, C.; Zografos, A.; Igglessi-Markopoulou, O. *Heterocycles* **1999**, *51*, 1543.
11. Phadtare, S. K.; Kamat, S. K.; Panse, G. T. *Indian J. Chem., Sect. B* **1983**, *22*, 496.
12. Chk1 inhibitory activity was measured using a homogeneous time-resolved fluorescence assay that detects phosphorylation of a biotinylated GSK-3 peptide as described by Barnett, S. F. et al. *Biochem. J.* **2005**, *385*, 399, The assay was run at 0.5 nM enzyme and 0.1 mM ATP. IC_{50} values are reported as averages of at least two independent determinations; standard deviations are within +25–50% of IC_{50} values..
13. NCI-H1299 lung carcinoma cells were arrested with 16 h treatment of camptothecin and then treated with Chk1 inhibitors for additional 8 h. Escape from cell cycle arrest and progression into mitosis due to Chk1 inhibition were measured by quantifying the mitosis-specific phosphorylation of nucleolin using an antibody-coated, bead-based assay. For assay details, see: Fraley, M. E. et al. *Bioorg. Med. Chem. Lett.* **2006**, *16*, 1775, Ref. 16. The values of EC_{50} were measured with 10-point, half-log dilution series and are reported as an average of tetraplicate determinations.
14. Potency enhancement via substitution at the 8-position of the pyrazoloquinolinone was also observed at the corresponding position of a series of indoles as noted in Palmer, B. D. et al. *J. Med. Chem.* **2006**, *49*, 4896; Prudhomme, M. et al. *Eur. J. Pharmacol.* **2007**, *554*, 106.
15. Note that in the enzyme assay, the Chk1 inhibitory activity is measured at K_m for ATP (0.1 mM). However, in the cell assay the ATP concentration is 2.0 mM resulting in an inherent 10-fold shift in potency between these assays.
16. Sridhar, R.; Sivaprasad, G.; Perumal, P. T. *J. Heterocyclic Chem.* **2004**, *41*, 405.
17. *N*,*N*,*N*′,*N*′-Bis(tetramethylene)-chloroformamidinium hexafluorophosphate.
18. We found it to be necessary to alkylate the amide in order for the Heck cyclization to proceed.
19. The 1-ethyl group was found not to be potency enhancing as shown in the comparison between compounds **1** and **8**.
20. (a) Papageorgiou, C.; Camensich, G.; Borer, X. *Bioorg. Med. Chem. Lett.* **2001**, *11*, 1549; (b) Huang, S. et al. *Bioorg. Med. Chem. Lett.* **2006**, *16*, 5907.
21. PSA was calculated by the method of Clark, D. E. *J. Pharm. Sci.* **1999**, *88*, 807.
22. Compounds **32** were prepared by treating **7** with $(Boc)_2O$ and catalytic DMAP in DMF at 23 °C.
23. Daou, B.; Soufiaoui, M. *Tetrahedron* **1989**, *45*, 3351.
24. The tetrahydronaphthyl aryl bromide anthranilic acid precursor was synthesized by the reduction of commercially available naphthyl anthranilic acid with Raney nickel, followed by bromination using Br_2 in pyridine in 85% overall yield.
25. Note that the Chk1 X-ray crystal structure with bound inhibitor **49** indicated a 2.80 Å bond length between the amine and side chain of Glu91.
26. At this stage of our optimization efforts, we became aware of independent efforts to optimize this series (WO2005028474).
27. Blockade of hERG has been implicated in the drug-induced alteration of cardiac ventricular repolarization that is typically manifested in prolongation of the heart rate-corrected QT interval (QT_c). Prolongation of QT_c interval may potentiate cardiac arrhythmia in patients and lead to torsades de pointes or sudden death. See: DePonti, F.; Poluzzi, E.; Cavalli, A.; Recanatini, M.; Montanaro, N. *Drug Safety* **2002**, *25*, 263.
28. The hERG IC_{50} values were determined by binding competition experiments using membrane preparations from human embryonic kidney cells that constitutively express hERG.
29. Jamieson, C.; Moir, E. M.; Rankovic, Z.; Wishart, G. *J. Med. Chem.* **2006**, *49*, 5029.
30. pK_a was calculated using Marvin software, available from ChemAxxon Ltd.
31. Bromides utilized in the synthesis of compounds **50**–**52** were generated from diethyl fluoromalonates via a multistep sequence; separation of enantiomers was carried out using chiral normal phase chromatography and assignment was based on an independent enantioselective synthesis.